THE JOURNAL OF BIOLOGICAL CHEMISTRY VOL. 285, NO. 35, pp. 26998–27007, August 27, 2010

Na^+-dependent HCO_3^- Import by the *slc4a10* Gene Product Involves Cl^- Export*

Received for publication, January 28, 2010, and in revised form, May 30, 2010 Published, JBC Papers in Press, June 21, 2010, DOI 10.1074/jbc.M110.108712

Helle Hasager Damkier[‡§1], **Christian Aalkjaer**[‡¶], **and Jeppe Praetorius**[‡§]

From the [‡]*Water and Salt Research Center,* [§]*Department of Anatomy, and* [¶]*Department of Physiology and Biophysics, Aarhus University, DK-8000 Aarhus, Denmark*

The *slc4a10* gene encodes an electroneutral Na^+-dependent HCO_3^- importer for which the precise mode of action remains unsettled. To resolve this issue, intracellular pH (pH_i) recordings were performed upon acidification in the presence of CO_2/HCO_3^- by 2′,7′-bis(carboxyethyl)-5,6-carboxyfluorescein (BCECF) fluorometry of stably *slc4a10*-transfected NIH-3T3 fibroblasts. *slc4a10* expression induced a significant Na^+-dependent pH_i recovery, which was accompanied by an increase in the intracellular Na^+ concentration evaluated by use of the Na^+-sensitive fluorophore CoroNa Green. The estimated Na^+:HCO_3^- stoichiometry was 1:2. Cl^- is most likely the counterion maintaining electroneutrality because (i) Na^+-dependent pH_i recovery was eliminated in Cl^--depleted cells; (ii) acute extracellular Cl^- removal led to a larger alkalization in *slc4a10*-transfected cells than in control cells; and (iii) the 4,4′-diisothiocyanato-stilbene-2,2′-disulfonic acid (DIDS)-sensitive and Na^+- and HCO_3^--dependent $^{36}Cl^-$-efflux during pH_i recovery was significantly greater in acidified *slc4a10*-transfected cells than in control cells. Charged amino acids specific to *slc4a* gene family members that transport Na^+ and are expected to move more HCO_3^- molecules/turnover were targeted by site-directed mutagenesis. Na^+-dependent pH_i recovery was reduced in each of the single amino acid mutated cell lines (E890A, E892A, H976L, and H980G) compared with wild type *slc4a10*-transfected cells and completely eliminated in quadruple mutant cells. In conclusion, the data suggest that *slc4a10* expressed in mammalian cells encodes a Na^+-dependent Cl^-/HCO_3^- exchanger in which four specific charged amino acids seem necessary for ion transport.

Tight control of intracellular pH (pH_i)[2] is crucial for maintaining a variety of basic cellular functions (1). Regulation of pH_i largely depends on acute intracellular buffering and longer term extrusion or import of acid/base equivalents. Integral plasma membrane proteins such as the Na^+-dependent HCO_3^- transporters from the solute carrier gene family 4 (*slc4a*) mediate these functions. The *slc4a10*-gene product is primarily expressed in the central nervous system and is important for normal brain function (2–4). In the choroid plexus, the *slc4a10* gene product is a main basolateral Na^+ loader and is most likely necessary for secretion of cerebrospinal fluid because disruption of the *slc4a10* in mice leads to decreased brain ventricle sizes (4). In humans, a mutation in the *SLC4A10* promoter region resulted in severe complex partial epilepsy and mental retardation (5).

Within the gene family, *slc4a10* shares the highest amino acid homology with the electroneutral Na^+:HCO_3^- cotransporter Nbcn1 (*slc4a7*) and the Na^+-dependent Cl^-/HCO_3^- exchanger, Ndcbe (*slc4a8*). The transport mode of the *slc4a10* gene product has been investigated by more research groups defining the protein as an electroneutral Na^+ and HCO_3^--dependent transporter which is inhibited by 4,4′-diisothiocyanatostilbene-2,2′-disulfonate (DIDS) (2, 6, 7). The studies, however, differ in opinion regarding the involvement of Cl^- in the transport process. Thus, the human *SLC4A10* gene product, first designated with the abbreviation Ncbe for Na^+-dependent Cl^-/HCO_3^- exchanger (2), was recently suggested renamed as Nbcn2 for electroneutral Na^+:HCO_3^- cotransporter 2, displaying Cl^-/Cl^- self-exchange instead of Cl^-/HCO_3^- exchange activity (7). The knowledge on the primary structure of the *slc4a10*-derived protein is not sufficient to suggest which parts of the transmembrane region are involved in ion translocation and can, thus, not help predict the mode of action for this Na^+-dependent HCO_3^- transporter. More structure-function data are available on the anion exchanger Ae1 (*slc4a1*), which seems to present two hinge-like loops within the transmembrane region with access to both the extra- and intracellular environment (8). These loops were proposed to be involved in attraction and perhaps even translocation of ions by Ae1.

In this investigation, we aimed to define the transport mode of the *slc4a10* gene product by analyzing the targeted ionic and structural requirements for transport by the protein. The study was conducted on mammalian NIH-3T3 fibroblasts devoid of endogenous Na^+-dependent HCO_3^- transport stably transfected with single copies of the coding region of rodent *slc4a10*. We found three lines of evidence for the functional involvement of Cl^- in transport by the *slc4a10*-derived protein: (i) the Na^+:HCO_3^- stoichiometry was estimated to 1:2; (ii) Na^+-dependent pH_i regulation was dependent on the presence and the

* This work was supported by the Danish Medical Research Council, Karen Elise Jensens Fond, the Lundbeck Foundation, Aarhus University Research Foundation, and the Novo Nordisk Foundation. The Water and Salt Research Center at Aarhus University was established and funded by the Danish National Research Foundation (Danmarks Grundforskningsfond).

[1] Supported by the Faculty of Health Sciences, Aarhus University. To whom correspondence should be addressed: Wilhelm Meyers Allé 3, DK-8000 Aarhus C, Denmark. Tel.: 45-8942-3008; Fax: 45-8619-8664; E-mail: hd@ana.au.dk.

[2] The abbreviations used are: pH_i, intracellular pH; BBS, bicarbonate-buffered saline; BCECF, 2′,7′-bis(carboxyethyl)-5,6-carboxyfluorescein; DIDS, 4,4′-diisothiocyanatostilbene-2,2′-disulfonate; FRT, flipase recognition target; HBS, HEPES-buffered salt solution; Nbcn, electroneutral Na^+;HCO_3^- cotransporter; Ncbe, Na^+-dependent Cl^-/HCO_3^- exchanger; Nbce, electrogenic Na^+;HCO_3^- cotransporter; Ndcbe, Na^+-dependent Cl^-/HCO_3^- exchanger; NPPB, 5-nitro-2-(3-phenylpropylamino)-benzoate; *Slc4a*, solute carrier family 4.

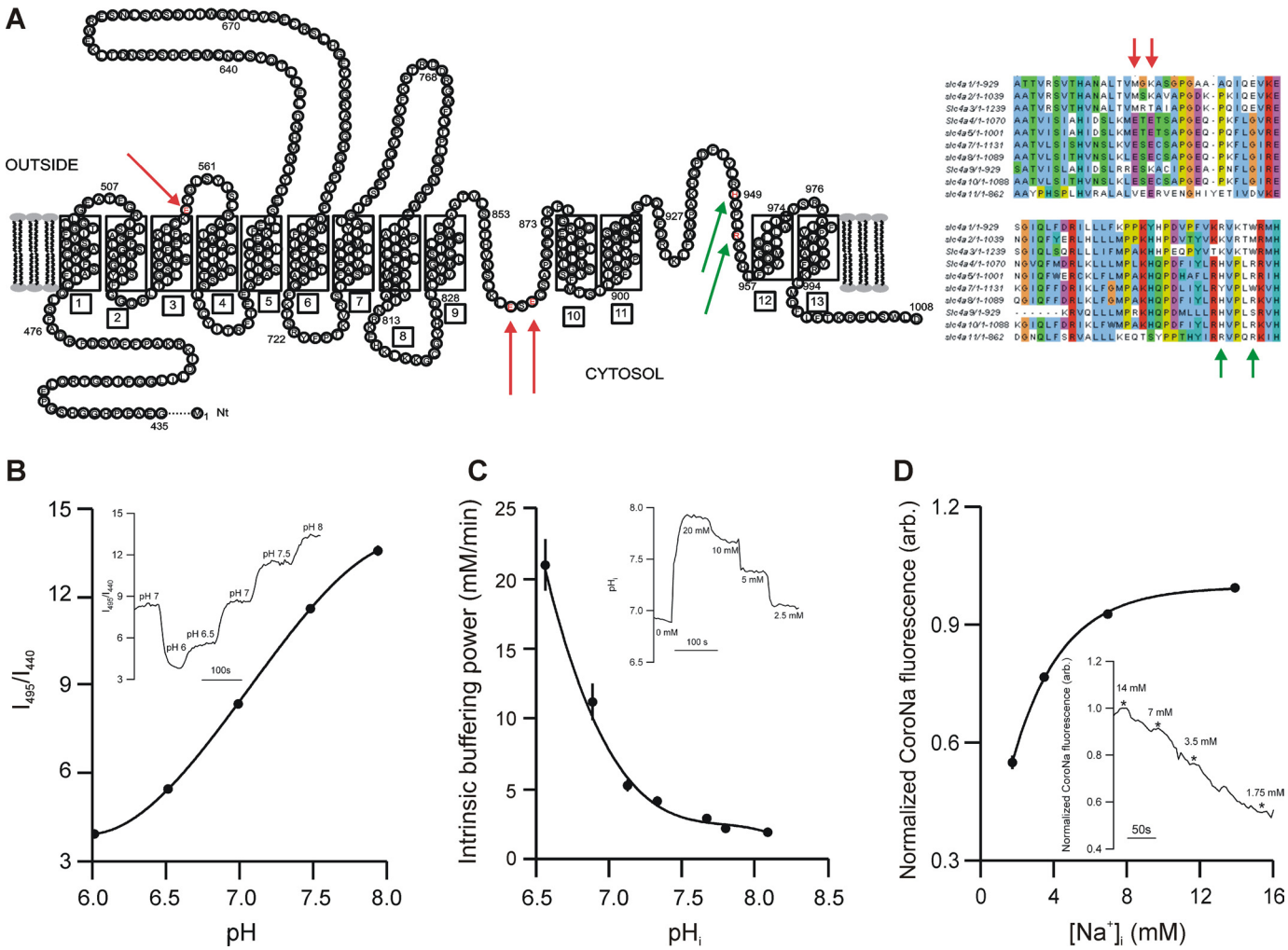

FIGURE 1. *A*, proposed topological model for the mouse *slc4a10*-derived polypeptide based on the similar model from *slc4a1*, Ae1. The mutated amino acids are highlighted in *red* and by *arrows*. *Right panels* show the amino acid alignment of the hinge-like loops of *slc4a*-derived polypeptides. Mutated amino acids are marked with *arrows*. (Modified with permission from J. Casey.) *B*, calibration of excitation fluorescence ratio (I_{495}/I_{440}) into pH_i values. *Inset* shows fluorescence ratio trace and extracellular pH values from one experiment. *C*, determination of pH_i buffering capacity, β_{int}. *Inset* shows pH_i trace and extracellular [$NH_4^+ + NH_3$] values from one experiment. *D*, calibration of intracellular CoroNa fluorescence to $[Na^+]_i$ values. *Inset* shows fluorescence recording and extracellular [Na^+] values from one experiment. *Error bars* = S.E.

gradient of Cl^-; and (iii) *slc4a10* transfection induced a DIDS-sensitive and HCO_3^--dependent increase in Cl^- efflux during Na^+-dependent pH_i regulation. Although there is a high degree of homology among the gene family members in the hinge-like regions, we aimed to identify amino acid residues of importance for transporter function based on bioinformatics and the literature on Ae1 mutagenesis. The analysis supports the importance of each of the four charged amino acids for Na^+:HCO_3^- import by the *slc4a10*-derived polypeptide. We recommend preserving the original name of the *slc4a10* gene product, Ncbe.

EXPERIMENTAL PROCEDURES

cDNA Constructs—The coding sequences of rat *slc4a10* (rb2Ncbe, NBCn2-D, AY579374) and mouse *slc4a10* (corresponding to rb1Ncbe, NBCn2-B, AB033759) were obtained by reverse transcription-PCR as described previously (9) and inserted into pcDNA5/FRT vectors (flipase recognition target; Invitrogen). The rat *slc4a7* (Nbcn1d) gene was purchased from Geneart (Regensburg, GE) and inserted into the same vector. Mutation sites in the *slc4a10* were chosen by comparative analysis of the predicted amino acid sequence in all members of the *slc4a* family and across the species: mouse, rat, dog, and human. The hinge-like loops of Ae1 have been suggested as sites for ion translocation. There are only four charged candidate amino acids in these domains and the flanking transmembrane domains of *slc4a*-derived polypeptides that vary systematically among the members of the gene family. Putative Na^+-attracting motifs in the hinge-like loop regions were identified as the negatively charged amino acids found in Na^+-dependent but not in Na^+-independent *slc4a* family members *i.e.* Ae1–4. Alanine substitutions were introduced at positions Glu^{890} and Glu^{892} (Fig. 1*A*) by site-directed mutagenesis (Stratagene). As negative control, a similar mutation was made in Glu^{584} just after the first transmembrane domain. Two putative anion-attracting motifs were selected based on the appearance of positively charged amino acids in the hinge-like loops. One amino acid is specific to *slc4a* family members believed to transport more than two HCO_3^- molecules/Na^+ (Nbce1, Nbce2, and Ndcbe). The other amino acid is charged in the anion exchangers, polar in Nbcn1 and has the pH-sensitive histidine in all

TABLE 1
Experimental solutions

Solution	HBS	0Na^+ / HBS	NH_4^+ / HBS	0Cl^- / HBS	HiK^+ / HBS	BBS	0Na^+ / BBS	NH_4^+ / BBS	0Cl^- / BBS	0NaCl / BBS
Na^+	145.0		125.0	145.0	10.0	145.0		125.0	145.0	
K^+	3.6	3.6	3.6	3.6	138.6	3.6	3.6	3.6	3.6	3.6
Ca^{2+}	1.8	1.8	1.8	1.8	1.8	1.8	1.8	1.8	1.8	1.8
Mg^{2+}	0.8	0.8	0.8	0.8	0.8	0.8	0.8	0.8	0.8	0.8
NH_4^+			20.0					20.0		
Cl^-	138.6	138.6	138.6		138.6	114.6	114.6	114.6		
SO_4^{2-}	0.8	0.8	0.8	0.8	0.8	0.8	0.8	0.8	0.8	0.8
HCO_3^-						24.0	24.0	24.0	24.0	24.0
Glucose	5.5	5.5	5.5	5.5	5.5	5.5	5.5	5.5	5.5	5.5
HEPES	10.0	10.0	10.0	10.0	10.0	10.0	10.0	10.0	10.0	10.0
NMDG		145.0					121.0			121.0
Gluconate				138.6					114.6	114.6
Choline							24.0			24.0
PO_4^{2-}	2.0	2.0	2.0	2.0	2.0	2.0	2.0	2.0	2.0	2.0
pH	7.4	7.4	7.4	7.4	7.4	7.4	7.4	7.4	7.4	7.4

other Nbcs. Mutations were introduced at positions His^{976} and His^{980} by replacing the histidines with leucine and cysteine, respectively. Resulting cDNA was sequenced and cloned into the pcDNA5/FRT vector. A construct encoding a nucleus-targeted red fluorescent protein, pDsRed2-Nuc (Clontech) was also cloned into that vector and used as a functionally negative control for *slc4a10* throughout this study.

Cell Culture—FRTs containing NIH-3T3 fibroblasts (Invitrogen) were grown in Dulbecco's modified Eagle's medium glutaMAX™ supplemented with 10% donor bovine serum. Cells were stably transfected with a single copy of cDNA constructs into a predefined locus using the Flp-In™ system (Invitrogen). Transfection and protein expression were validated by PCR and sequencing, surface biotinylation, Western blotting, and immunocytochemistry.

Fluorophores—For pH_i measurements, cells were loaded in 2 μM BCECF-AM in a HEPES-buffered salt solution (HBS; Table 1) for 15 min. For intracellular $[Na^+]$ measurements, cells were loaded in 10 μM CoroNa Green sodium indicator for 30 min in HBS. All incubations were performed in a dark chamber heated to 37 °C. Fluorophores were purchased from Invitrogen.

Intracellular pH and $[Na^+]$ Measurements—Cells were grown to approximately 50% confluence on glass coverslips. Fluorophore-loaded cells were mounted in a closed perfusion chamber (358-μl RC-21BR or 36-μl RC-20; Warner Instruments) and perfused with a linear flow rate of 0.8 mm/s at 37 °C. For pH_i measurements, the dye excitation periods of 20 ms were alternating between 495-nm and 440-nm light from a monochromator (Till Photonics). The light emission at 510–535 nm was recorded by a 12-bit cooled monochrome CCD camera (QImaging, Retiga EXi). QED InVivo imaging software (Media Cybernetics) was used to control wavelength, light exposure time (20 ms), frequency (one image pair each 4 s), and 4×4 binning (to 348×260 pixel images), as well as the data collection from regions of interest (one/individual cell). The mean values for cells from one coverslip represent $n = 1$. Where indicated, fluorophore-loaded cells were mounted in a coverslip holder and placed in a cuvette containing experimental solution in a heated cuvette house as alternative to fluorescence microscopy. For pH_i measurements, dye excitation alternated between 495-nm and 440-nm monochromator light at 1 Hz, and the light emission at 510–535 nm was recorded by a photomultiplier tube of a Quantum Master UV-visual QM-4 spectrofluorometer (Photon Technologies International). The ratio derived from the BCECF measurements was calibrated to intracellular pH_i by clamping intracellular pH to stepwise changing extracellular pH by 10 μM nigericin in a high K^+ buffer (10) (Fig. 1*B*). The Na^+-dependent $d[H^+]_i/dt$ was calculated as the product of dpH_i/dt and the total buffering power, β_{tot}. The β_{tot} was calculated as the sum of the intrinsic buffering power (β_{int}) and the contribution of the CO_2/HCO_3^- buffering system as previously described (10, 11) (Fig. 1*C*). For the single wavelength $[Na^+]_i$ dye CoroNa Green, the excitation/emission wavelengths were 492/516 nm. CoroNa fluorescence was calibrated to $[Na^+]_i$ values by varying extracellular $[Na^+]$ in the presence of the ionophore monensin, 10 μM (Fig. 1*D*). Each time course recording was followed by a one-point calibration of $[Na^+]_i$ to 14 mM with monensin. The changes were fully reversible, and neither photobleaching nor probe leak was observed during the experiments. The composition of experimental solutions is listed in Table 1.

$^{36}Cl^-$ Flux Measurements—Cells were grown to 80% confluence in 12-well plates (Life Sciences) and loaded with 2 μCi/ml $H^{36}Cl$ (added equimolar amount of NaOH) or $Na^{36}Cl$ in HBS for 2 h in a heating chamber at 37 °C (GE Healthcare or Risø National Laboratory, Denmark, respectively). Cells were acidified for 3 min by adding NH_4Cl to the solution (final concentration 20 mM) and washed four times in a Na^+-free CO_2/HCO_3^--buffered salt solution. The last wash was added 125 μM of the Cl^- channel blocker 5-nitro-2-(3-phenylpropylamino)-benzoate, NPPB, and was collected for scintillation counting. After the final wash, the cells were incubated with Na^+-containing BBS with the same Cl^- channel blocker. The solution was collected for scintillation counting after 2 min. In parallel wells, 200 μM DIDS was added to block *slc4a10* gene product activity in the continued presence of the Cl^- channel blockers. To compare values between wells of varying cell density, we normalized the counts for the background Cl^- in the final wash in Na^+-free BBS. For assessment of intracellular Cl^- depletion, cells were loaded with $^{36}Cl^-$ as described above. After two washes in HBS, cells were incubated in Cl^--free HBS for 0, 1, 5 or 30 min before removal of the supernatant. After 2 washes in Cl^--free HBS and addition of 0.2 M NaOH, the cell lysates were collected for scintillation counting. Cl^- influx was measured by

exposing cells to 8 μCi/ml $Na^{36}Cl$ for 2 min corresponding to the initial period of Na^+-dependent pH_i recovery after NH_4Cl prepulsing in the presence of 1 mM furosemide. Cells were washed three times in cold HBS before lysis and counting. The influx values were corrected for variations in cell number (^3H_2O space). All samples were run in duplicate and measured in a liquid scintillation counter (RackBeta 1211; LKB Wallac). The Cl^- efflux rate constants were determined as fractional loss of isotope/min.

Immunocytochemistry—Cell cultures were fixed and immune-stained as described previously (12). In brief, 50–75% confluent cells were fixed in 4% paraformaldehyde in phosphate-buffered solution (PBS: 167 mM Na^+, 2.8 mM $H_2PO_4^-$, 7.2 mM $H_2PO_4^{2-}$, pH 7.4), permeabilized in 0.2% saponin, and blocked in 10% FCS, 0.1% BSA, and 0.05% saponin in PBS. After additional blocking with 1% BSA, 0.2% fish gelatin, 0.05% saponin, and 0.05 M glycine in PBS, cells were stained with anti-*slc4a10* antibody (3, 9) in PBS with 0.5% BSA and 0.05% saponin and then incubated with Alexa Fluor 488 goat anti-rabbit IgG (Invitrogen). Cells were counterstained using Topro3 nuclear stain (Invitrogen).

Surface Biotinylation and Immunoblotting—Stably transfected cells were grown to 80% confluence in 25-cm^2 surface area flasks. Cell surface biotinylation was achieved by adding biotin to washed cells at 4 °C as detailed previously (13). After cell lysis and sonication, the biotinylated proteins from the cleared homogenate were isolated using a neutravidin column. Eluates from the columns were added 1.5% (w/vol) SDS, 40.0 mM 1,4-dithiothreitol, 6% (v/v) glycerol, 10 mM Tris(hydroxymethyl)-aminomethane, pH 6.8, and bromphenol blue. Samples were heated for 15 min at 65 °C and stored at 4 °C until use. Proteins were separated by SDS-PAGE (12). Proteins were then electrotransferred onto nitrocellulose membranes and blocked by 5% nonfat dry milk in a Tween-containing PBS. The membranes were incubated with the same primary antibody as above and subsequently with horseradish peroxidase-conjugated goat anti-rabbit IgG secondary antibody (Dako, Glostrup, Denmark). The signal was detected by an ECL kit (Amersham Biosciences).

Statistical Analysis—In general, data were analyzed by two-tailed *t* test using GraphPad Instat software. An analysis of variance test with Dunnett *post hoc* test was performed for multiple comparisons of unpaired pH_i recoveries. A paired, nonparametrical analysis of variance test (Friedman) was performed for surface biotinylation data, where Gaussian distribution could not be expected. Values of $p < 0.05$ were considered an appropriate level of statistical significance.

RESULTS

slc4a10-transfected Cells Display Na^+-dependent pH_i Recovery and Na^+ Import following Acidification—The Na^+:HCO_3^- transport capacity of rat *slc4a10*-transfected cells was investigated by pH_i measurements. The *slc4a10*-transfected cells exhibited significant Na^+-dependent pH_i recovery following NH_4Cl-induced acidification compared with the dsRed-transfected negative controls (Fig. 2*A*; pH_i acidification level *slc4a10*, 6.29 ± 0.07; dsRed, 6.22 ± 0.05, $n = 6$, not significant). As expected for a Na^+:HCO_3^- transporter, the activity was fully dependent on the presence of CO_2/HCO_3^- and was blocked by 200 μM DIDS (Fig. 2*B*). An unexpected Na^+/H^+ exchange activity was induced by transfection with both *slc4a10* and dsRed. This transport was inhibited by 5-(*N*-ethyl-*N*-isopropyl) amiloride during pH_i recoveries in all experiments. In parallel to the pH_i recovery, there was a significant increase in $[Na^+]_i$ in *slc4a10*-transfected cells compared with the control cells (Fig. 2*C*).

slc4a10-transfected Cells Transport Na^+ and HCO_3^- with an Apparent Stoichiometry of $1Na^+$:$2HCO_3^-$—To estimate the stoichiometry of the Na^+:HCO_3^- transport, pH_i and $[Na^+]_i$ were measured after NH_4Cl prepulsing in smaller perfusion chambers to increase the fluid exchange rate (Fig. 3*A*, *left* and *center panels*, respectively). The net pH_i recovery rate and $[Na^+]_i$ change were determined the first 20 s after returning acidified cells to Na^+-containing CO_2/HCO_3^--buffered solution and subtracted the corresponding values obtained in dsRed-transfected cells. The experiments indicate that 1.93 acid/base equivalents are transported for each Na^+ molecule (Fig. 3*A*, *right panel*, $p = 0.002$, $n = 6$). To establish the accuracy of this estimate, the measurements were repeated by cuvette-based fluorometry in which a larger number of cells are measured simultaneously and with virtually instantaneous fluid exchange (Fig. 3*B*). The pH_i recovery rate and $[Na^+]_i$ change were determined the first 5 s after returning acidified cells to Na^+-containing CO_2/HCO_3^--buffered solution and subtracting the corresponding values obtained in dsRed-transfected cells. The experiments suggested a Na^+:HCO_3^- stoichiometry of 1:2.19 (Fig. 3*C*, *left panel*, $p = 0.001$, $n = 6$). The same cell culture line transfected with the *slc4a7* gene (Nbcn1) also displayed Na^+-dependent pH_i recovery and corresponding $[Na^+]_i$ changes. With the same method and data analysis, the apparent Na^+:HCO_3^- stoichiometry for Nbcn1 was 1:1.17 (Fig. 3*C*, *right panel*, $n = 6$).

$Na^+HCO_3^-$ Transport in slc4a10-transfected Cells Is Dependent on the Presence of Cl^-—The Na^+:HCO_3^- stoichiometry estimates suggest that a negative counterion or a positive cotransported ion is needed to maintain electroneutrality. Cl^- has previously been suggested as the negative counter ion for the *slc4a10* gene product. To remove both intracellular and extracellular Cl^-, the *slc4a10*-transfected cells were incubated in the absence of extracellular Cl^- for 30 min prior to pH_i measurements. Cells were acidified by the addition of 20 mM propionate/propionic acid to the BBS (Fig. 4*A*), as the cells did not acidify by NH_4^+ prepulsing in the absence of Cl^-. The Na^+-dependent pH_i recovery of the Cl^--depleted rat *slc4a10*-transfected cells was dramatically decreased compared with cells with normal Cl^- content (Fig. 4*B*, $p = 0.0002$, $n = 6$, initial pH values for *slc4a10* in the absence of Cl^-: 6.75 ± 0.05 *versus* 6.74 ± 0.05 in the presence of Cl^-). The Na^+:HCO_3^- transport activity was decreased to the level observed in dsRed-transfected control cells. Depleting dsRed-transfected cells of Cl^- prior to pH_i measurements did not further inhibit Na^+-dependent pH_i recovery ($n = 6$, not significant; initial pH values in Cl^--depleted dsRed-transfected cells: 6.78 ± 0.05 *versus* 6.75 ± 0.06 in the presence of Cl^-). Cl^- depletion was assessed by cellular loss of $^{36}Cl^-$. After Cl^- loading, cells gradually lost intracellular Cl^- tracer to a level close to background count

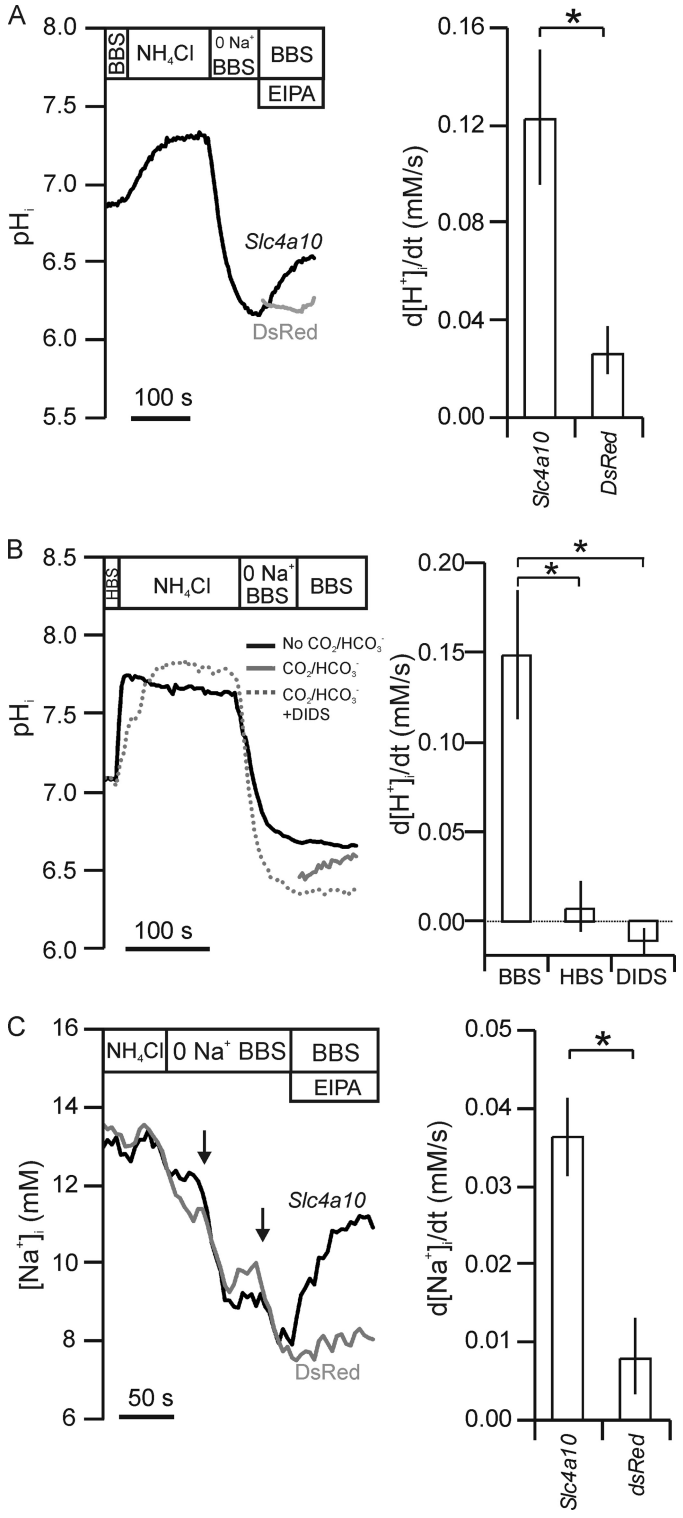

FIGURE 2. **Na^+ and HCO_3^- import in stably rat *slc4a10*-transfected NIH-3T3 cells.** *A*, example of pH_i recording from BCECF-loaded *slc4a10*-transfected (*black*) and negative control dsRed-transfected cells (*gray*) by fluorescence microscopy. Cells were acidified by a 20 mM NH_4Cl prepulse followed by a wash in Na^+-free solution in larger volume perfusion chambers. The pH_i recovery rates ($d[H^+]_i/dt$) were determined from the curve slope after readdition of Na^+. *Bar graph* shows mean $d[H^+]_i/dt$ values ± S.E. (*error bars*) of six such experiments. *B*, recording of pH_i changes during NH_4Cl prepulsing and recovery after acidification in the presence and absence of CO_2/HCO_3^- and with the inhibitor DIDS in BBS. *Bar graph* shows mean values ± S.E. of similar experiments on *slc4a10*-transfected cells in the presence and absence of CO_2/HCO_3^- (BBS and HBS, respectively) or with the inhibitor DIDS in BBS, 200 μM (*n* = 5). *C*, $[Na^+]_i$ recordings in CoroNa Green-loaded *slc4a10*-transfected (*black*) and negative control cells (*gray*). The rate of change in intracellular Na^+ concentration ($d[Na^+]_i/dt$) was determined after readdition of Na^+. *Arrows* indicate focus adjustment. *Bar graph* represents mean $d[Na^+]_i/dt$ values ± S.E. of six experiments. *Error bars* = S.E.

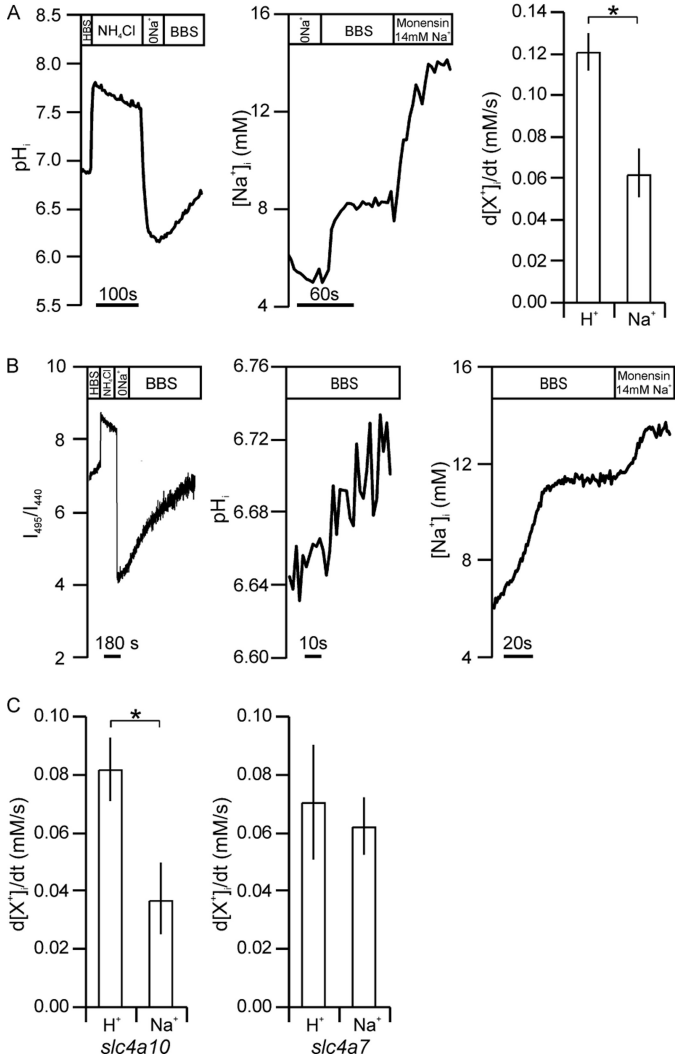

FIGURE 3. **Estimations of $Na^+HCO_3^-$ stoichiometry for *slc4a10*- and *slc4a7*-transfected cells.** *A*, pH_i recording of BCECF-loaded *slc4a10*-transfected cells by fluorescence microscopy using fast exchange perfusion chambers (*left panel*). *Center panel*, corresponding $[Na^+]_i$ recordings in acidified CoroNa Green-loaded *slc4a10*-transfected cells. *Right panel*, mean $d[X^+]_i/dt$ values ± S.E. (*error bars*), where X^+ refers to H^+ and Na^+, as indicated (*n* = 6). *B*, *left panel*, cuvette fluorometry trace with the coverslip placed in a cuvette throughout the experiment. *Center* and *right panels*, traces of Na^+-dependent pH_i recoveries (*center panel*) and $[Na^+]_i$ changes (*right panel*) upon acidification of *slc4a10*-transfected cells where acidification was performed before transfer to the cuvette. *C*, mean $d[Na^+]_i/dt$ values and $d[H^+]_i/dt$ values ± S.E. of *slc4a10*-transfected cells (*left panel*, *n* = 6) and *slc4a7*-transfected cells (Nbcn1, *right panel*, *n* = 6) corrected for the corresponding values from dsRed-transfected cells. *, statistical significance. *Error bars* = S.E.

after 30 min (Fig. 4*C*). These experiments indicate that the 30-min Cl^--free incubation was sufficient to deplete the cells of Cl.

Na^+ HCO_3^- Transport in slc4a10-transfected Cells Is Sensitive to the Transmembrane Cl^- Gradient—The Cl^- requirement for Na^+ and HCO_3^- import by the rat *slc4a10* gene product was further investigated by creating an outward Cl^-

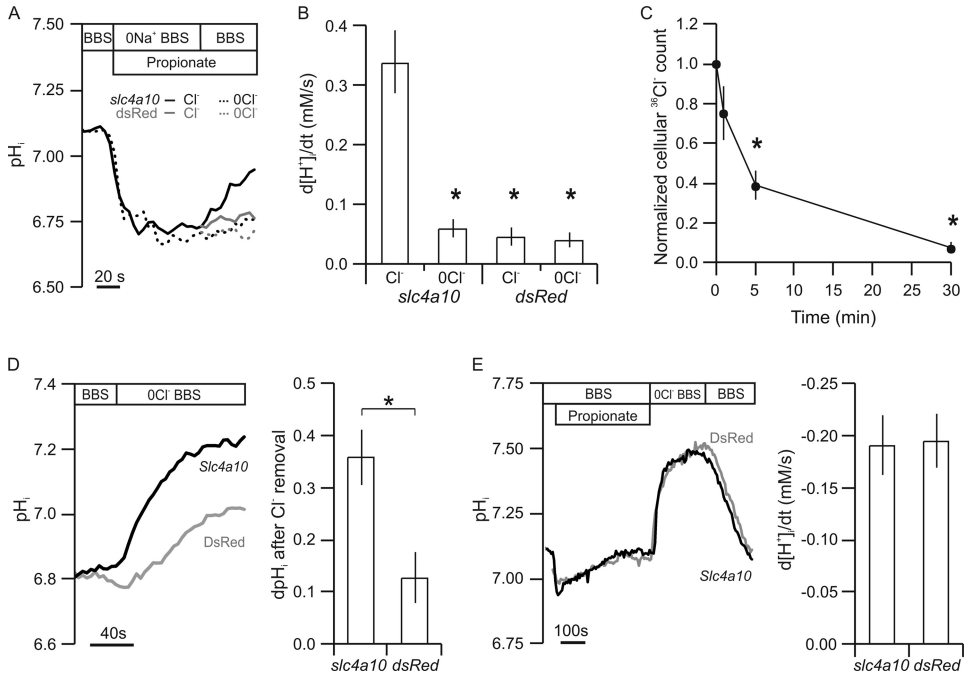

FIGURE 4.**The *slc4a10* polypeptide is Cl^--dependent and sensitive to the Cl^- gradient.** *A*, pH_i recordings from *slc4a10*-transfected (*black*) and negative control cells (*gray*) by fluorescence microscopy. Cells were depleted of Cl^- for 30 min prior to the experiment by incubation in Cl^--free solution. Cells were acidified by addition of 20 mM propionate/propionic acid to a Na^+-free solution. The Na^+-dependent pH_i recovery rate was determined after the readdition of Na^+, as indicated. *B*, *bar graph* showing mean values ± S.E. (*error bars*) of $d[H^+]_i/dt$ ($n = 6$). *C*, time course of cellular Cl^- depletion from $^{36}Cl^-$-loaded cells upon removal of the ion from the extracellular medium. *D*, pH_i recordings of *slc4a10*-transfected (*black*) and negative control cells (*gray*) by fluorescence microscopy, where Cl^- was removed from the extracellular medium as indicated. *Bar graph* shows the mean values ± S.E. of the maximal change in pH_i ($n = 6$). *E*, rat *slc4a10*-transfected and control cells alkalized by propionic acid (20 mM added to solution) prepulsing and the Cl^--dependent pH_i recovery rate determined. *Bar graph* shows the mean values ± S.E. of the pH_i recovery rates. *Error bars* = S.E.

gradient from the cells. An outward chemical Cl^- gradient is expected to induce Na^+:HCO_3^- import and thereby to induce intracellular alkalization in the case Cl^- is exported by the transporter in *slc4a10*-transfected cells. The alkalization resulting from the acute removal of Cl^- was significantly greater in *slc4a10*-transfected cells than the dsRed-transfected cells (Fig. 4*D*, initial pH_i values in the rat *slc4a10*-transfected cells: 6.81 ± 0.08 *versus* 6.71 ± 0.04 in dsRed-transfected cells, $p = 0.28$, $n = 6$). The same pattern was observed in mouse *slc4a10*-expressing cells (dpH_i in mouse *slc4a10*-expressing cells: 0.36 ± 0.05 *versus* dsRed-transfected cells: 0.07 ± 0.07, $p = 0.012$, $n = 5$). The alkalization observed in the dsRed-transfected cells most likely results from the reversed activity of an endogenous anion exchanger (*i.e.* HCO_3^- import and Cl^- extrusion). Thus, the anion exchange capacity of the cell lines was compared to ascertain that the observed difference in alkalization between the *slc4a10*- and dsRed-transfected cells represents *slc4a10*-induced HCO_3^- import. The anion exchanger activity was investigated at high pH_i at which forward anion exchange is favored and Na^+:HCO_3^- import is minimal. The alkalization was achieved by prepulsing the cells for 5 min by adding propionate/propionic acid followed by a shift to Cl^--free solution in the continued presence of CO_2/HCO_3^-. The Cl^- was reintroduced after a steady-state pH_i value had been reached, and the following pH_i change was determined as a measure for anion exchange activity. There was no statistical difference in anion exchange activity between the *slc4a10*- and dsRed-transfected cells (Fig. 4*E*; for anion exchange: $p = 0.914$, $n = 5$; initial pH values for *slc4a10*: 7.35 ± 0.03 *versus* 7.42 ± 0.05 for dsRed, $p = 0.28$).

slc4a10-transfected Cells Exhibit DIDS-sensitive $^{36}Cl^-$ Efflux after Acidification—Direct evidence for Cl^- transport by membrane proteins has classically been obtained by measuring $^{36}Cl^-$ transport. Cl^- efflux rate constants were determined during recovery from NH_4Cl-induced acidification to assess Cl^- extrusion during high rate Na^+ and HCO_3^- import. The $^{36}Cl^-$ efflux was computed before and after the readdition of Na^+ in the presence of the Cl^- channel blocker NPPB with and without DIDS. The Na^+-dependent $^{36}Cl^-$ efflux was significantly lower in the presence than in the absence of DIDS in the mouse *slc4a10*-transfected cells (Fig. 5*A*; $p = 0.02$, $n = 5$), but not in *dsRed*-transfected cells ($p = 0.21$, $n = 4$). The Na^+-dependent DIDS-sensitive dCl^-/dt can be calculated to 0.13 mM/s by multiplying the DIDS-sensitive rate constant of 0.4 min^{-1} by an estimated $[Cl^-]_i$ of 20 mM. Although this number may be inaccurate, it is in the same order of magnitude as the dNa^+/dt and dH^+/dt determined above. DIDS sensitivity of the Na^+-dependent Cl^- efflux during pH_i recovery from acidification was verified in another series of experiments (Fig. 5, *B–D*). In the absence of CO_2/HCO_3^-, the rate constant of the *slc4a10* polypeptide equaled the value in the presence of DIDS and CO_2/HCO_3^- (Fig. 5*B*). This indicated that the Cl^- efflux not only depends on Na^+, but is dependent on HCO_3^- as well. The values were corrected for the corresponding Na^+-independent Cl^- efflux rate constant from the same experiment (0.70 ± 0.13 in Na^+-free HBS, 0.67 ± 0.15 in Na^+-free BBS, $n = 5$, not significant). As a control, the corrected Cl^- efflux rate constants were also estimated for cells transfected with the Cl^--independent Nbcn1 or *dsRed* under identical circumstances (Fig. 5, *C* and *D*, respectively). We did not observe statistically significant differences in rate constants under the three experimental conditions for Nbcn1- or *dsRed*-transfected cells. Under identical experimental conditions, the Cl^- influx in *slc4a10*-transfected cells was not increased by the addition of CO_2/HCO_3^-. The values were practically identical to those of *slc4a7*-transfected cells (Fig. 5, *E* and *F*; baseline cpm over background in HBS *slc4a10*: 35.57 ± 13.56; *slc4a7*: 42.40 ± 16.72, not significant). These values most likely corresponds to the baseline Cl^- influx in HBS, as this influx was tripled in the same cell lines when the Na^+,K^+,$2Cl^-$ cotransport inhibitor furosemide was omitted from the solution (mean baseline cpm: 44 with furosemide and 138 without furosemide).

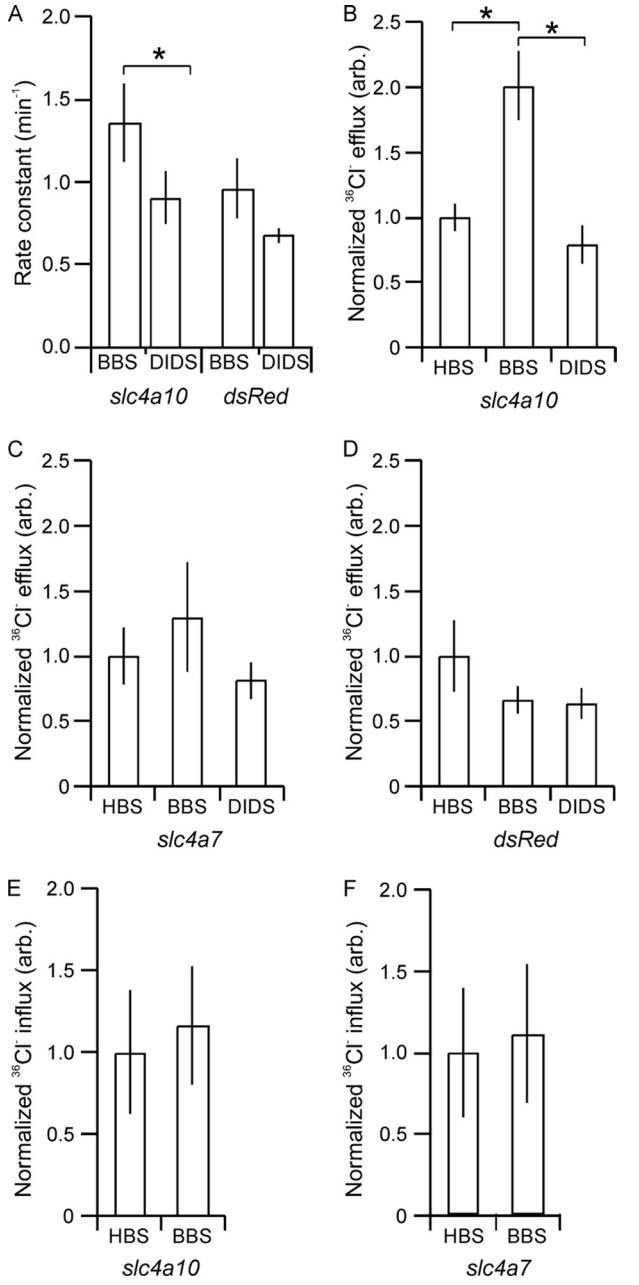

FIGURE 5. **The *slc4a10* polypeptide mediates Cl^- efflux but not Cl^- influx.** *A*, mean rate constants for the $^{36}Cl^-$ efflux of mouse *slc4a10*-transfected and control cells during the first 2 min after readdition of Na^+ to acidified cells in the absence (BBS) and the presence of DIDS. The difference in apparent rate constants between the columns for each cell line represents the Na^+-dependent DIDS-sensitive change in Cl^- per time unit ($n = 5$). *B*, similar experiments performed on cells transfected with *slc4a10* in presence/absence of CO_2/HCO_3^- and DIDS. Rate constants were normalized to the value obtained in the absence of HCO_3^-. These $^{36}Cl^-$ efflux measurements were run in parallel with *slc4a7*-transfected cells (*C*) and *dsRed*-transfected cells (*D*). In separate experiments, $^{36}Cl^-$ influx was measured for the first 2 min of pH_i recovery after acidification in cells transfected with *slc4a10* (*E*) or *slc4a7* (*F*) in the presence/absence of CO_2/HCO_3^-. *, statistical significance.

Specific Charged Amino Acids Are Necessary for Normal slc4a10-induced Transport—Mutations in mouse *slc4a10* were introduced at putative cation and anion attracting sites, selected as detailed under "Experimental Procedures." In brief, all charged amino acids in the proposed hinge-like loops of *slc4a10* that vary systematically among the gene family members were exchanged for uncharged amino acids (Glu^{890}, Glu^{892}, His^{976}, and His^{980}). In addition, a negatively charged amino acid outside these domains was mutated as well (Glu^{584}). The Na^+-dependent pH_i recovery profiles of cell lines stably transfected with mutant *slc4a10* forms were compared with the wild type *slc4a10*-transfected cell line (Fig. 6*A*). The pH_i recovery rate was reduced by 62–76% (range) in E890A, E892A, H976L, and H980G single amino acid mutations compared with wild type *slc4a10* cells (Fig. 6*B*, $p < 0.001$, $n = 5$), whereas transport was unaffected in the E584A cell line ($p = 0.70$, $n = 5$). We note that the Na^+-dependent pH_i recovery in wild type mouse *slc4a10*-transfected cells was similar to that of rat *slc4a10*-transfected cells (Fig. 6*B*). Quadruple E890A/E892A/H976L/H980G mutation as well as double E890A/E892A and H976L/H980G mutation eliminated pH_i recovery (quadruple: $p = 0.0002$, $n = 5$, E890A/E892A: $p = 0.002$, $n = 5$; H976L/H980G: $p = 0.002$, $n = 5$; Fig. 6*C*). For each mutant cell line, immunoblotting analysis of surface biotinylated *slc4a10* gene product was normalized to actin content of cell homogenate (to correct for cell density in culture flasks). There was no significant difference in surface *slc4a10* protein to actin ratio among the mutants and wt cells (Fig. 6*D*, range 0.7 to 1.7 of wt *slc4a10*, $n = 4$, $p > 0.05$). Fig. 5*E* shows representative micrographs of *slc4a10*-transfected NIH-3T3 cells used in the above experiments.

DISCUSSION

Na^+-driven HCO_3^- import is necessary for multiple cell types to maintain a suitable intracellular milieu and to mediate a transcellular transport of base equivalents in specialized epithelia. The integral membrane proteins responsible for this Na^+:HCO_3^- cotransport all belong to the solute carrier family 4, *slc4a*. Some controversy exists regarding the transport mode of one of these Na^+-dependent HCO_3^- transporters, the *slc4a10* gene product. Originally, the protein was characterized as a Na^+-dependent Cl^-/HCO_3^- exchanger, Ncbe (2), but a recent report suggested renaming the protein to Nbcn2 because Cl^- transport was not linked to the HCO_3^- transport (7). *slc4a10* disruption leads to (i) impaired regulation of intracellular pH upon acidification in the choroid plexus and hippocampal neurons, (ii) decreased brain ventricle volume, indicating abnormal cerebrospinal fluid formation, and (iii) increased seizure threshold (4). Because a human mutation in the *SLC4A10* has been reported to induce a severe phenotype (5), we believe it crucial to explore the nature of this gene product further.

There is agreement in the literature on the most basic transport characteristics of the *slc4a10* gene product. The Na^+ dependence of the *slc4a10*-induced pH_i regulation presented here is in accordance with all three previous studies characterizing the gene product (7, 2, 6). We show that intracellular [Na^+] actually increases during the pH_i recovery, providing direct evidence for the involvement of Na^+ import by the transporter. This concurs with the $^{22}Na^+$ uptake into untagged *SLC4A10*-injected *Xenopus* oocytes observed only in the presence of HCO_3^- (2). To propose amino residues that may be involved in Na^+ attraction and translocation, we mutated both negative amino acids in the loops that are shared by Na^+-trans-

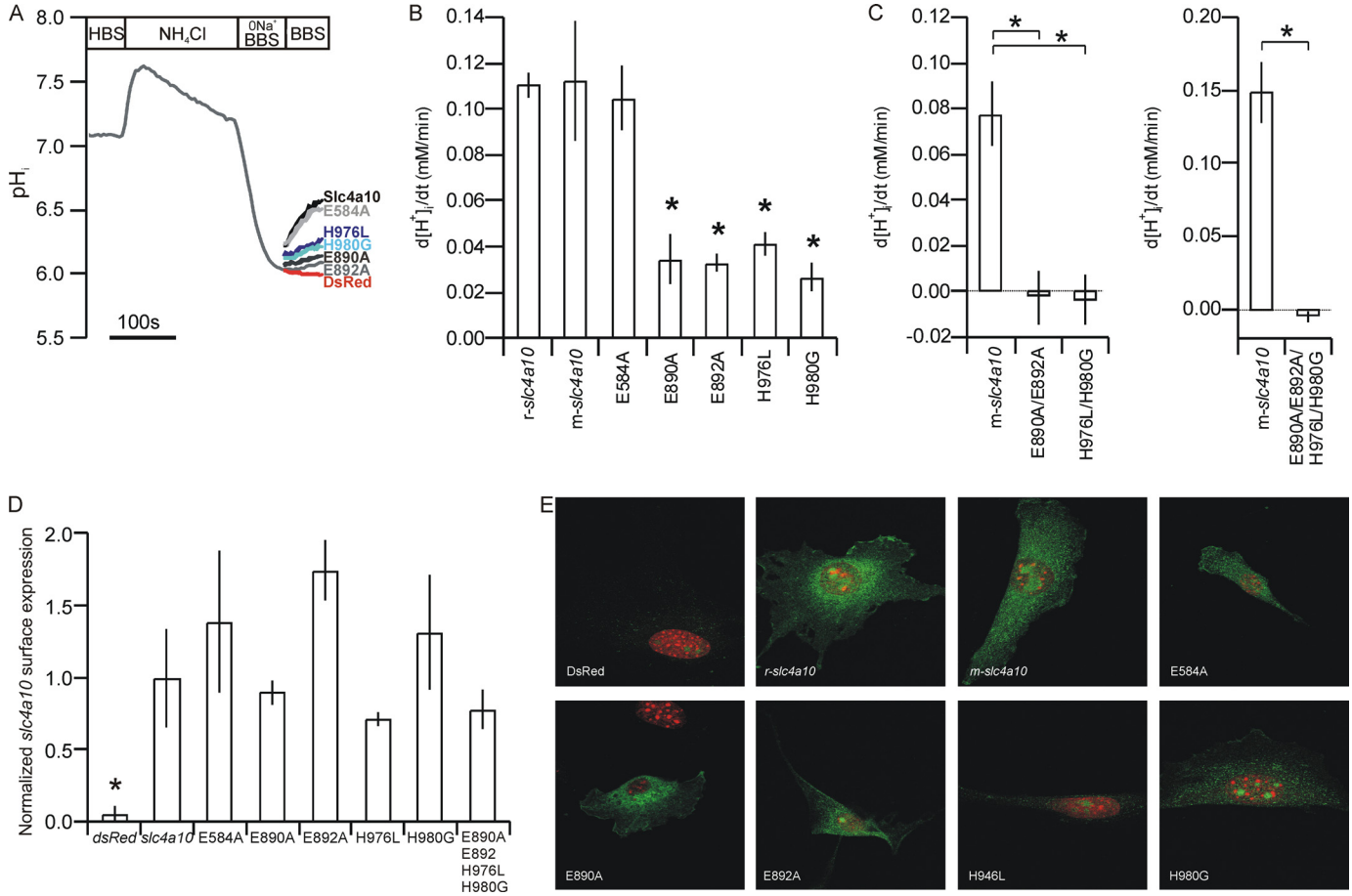

FIGURE 6. **Na^+-dependent HCO_3^- transport by the mouse *slc4a10* gene product after selective mutagenesis.** Mutations of *slc4a10* were introduced by site-directed mutagenesis in positions E584A, E890A, E892A, H976L, and H980G. Cell lines expressing each of these mutant forms were generated, and the Na^+-dependent HCO_3^- transport was assessed. *A*, pH_i recordings from wild type and mutated *slc4a10*-transfected and negative control cells (dsRed) by fluorescence microscopy. Cells were acidified by a 20 mM NH_4Cl prepulse followed by a wash in Na^+-free solution as indicated. The pH_i recovery rates ($d[H^+]_i/dt$) were determined from the slope after readdition of Na^+. *B*, mean $d[H^+]_i/dt$ values ± S.E. (*error bars*) after acidification of wild type *slc4a10* and formation of a single mutant *slc4a10* ($n = 5$). *C*, mean values ± S.E. of the Na^+-dependent pH_i recovery rate after acidification in double E890A/E892A, double H976L/H980G, and quadruple E890A/E892A/H976L/H980G *slc4a10*-mutants. *, statistical significance. *D*, immunoblot analysis of *slc4a10* protein expression after surface biotinylation. Cells were biotinylated on ice and surface proteins isolated on a neutravidin column. Immunoblotting these samples for *slc4a10* protein was corrected for cell density by actin immunoblots of the corresponding cell homogenates. *Bar graph* shows the mean values ± S.E. of the surface *slc4a10* protein/cell actin relation after normalization to mouse-*slc4a10* ($n = 4$). *E*, immunocytochemical micrographs of dsRed-transfected cells, wild type, and mutant *slc4a10*-transfected cells, as indicated. *Error bars* = S.E.

porting *slc4a*-derived proteins. By homology to the Ae1 protein, the Glu^{584} is located in the end of TM1, which is most unlikely to represent a flexible part of the protein. This mutation served as a negative control. In contrast, Glu^{890} and Glu^{892} are situated in the first putative hinge-like loop between the proposed TM9 and TM10, previously suggested to be involved in ion translocation in Ae1 (8). No other candidate amino acids could be deduced from the primary structures of *slc4a* genes. We found that mutation of only the two latter decreased *slc4a10*-induced Na^+-dependent pH_i recovery, which makes us speculate whether the amino acids may be involved in attracting or even translocating Na^+. Double mutation of these sites prevented pH_i recovery. To our knowledge, these amino acids have not been mutated in studies of other *slc4a* polypeptides, including Ae1. Apart from actual transport of Na^+, the present study also verifies the previous three investigations in the absolute requirement for CO_2/HCO_3^- and places the *slc4a10* product within the group of DIDS-sensitive Na^+-dependent HCO_3^- transporters.

The major discrepancies regarding the transport mediated by the *slc4a10* gene product seems to be the possible dependence and/or transport of Cl^-. Wang *et al.* found that HCO_3^- import after acidification in transiently *SLC4A10*-transfected HEK cells was virtually absent after 1-h Cl^- depletion (*i.e.* internal and external Cl^--free) (2). Giffard *et al.* (6) found the same using stably FLAG-tagged rat *slc4a10*-transfected NIH-3T3 cells after 20-min Cl^- depletion. This demonstrates either that the protein transports Cl^- or that it is merely sensitive to the presence of Cl^-. Evidence for direct Cl^- transport by the protein came from the demonstration of *SLC4A10*-induced Cl^- efflux which was DIDS-sensitive and dependent on Na^+, Cl^-, and HCO_3^- (2). Furthermore, long term equilibration at various extracellular [Cl^-] yielded a linear correlation between [Cl^-] and Na^+ uptake in *SLC4A10*-injected *Xenopus* oocytes in the same study. In contrast to this and the present work, Parker et al. (7) found that pH_i recovery is independent of Cl^- even after 20 min under Cl^--free conditions and that enhanced GFP-tagged *SLC4A10*-induced Cl^- efflux was independent of

extracellular Na^+. However, the authors do observe Na^+-driven Cl^-/HCO_3^- exchange in the absence of extracellular Cl^-. Finally, the lack of net Cl^- extrusion induced by *SLC4A10* was demonstrated in the same study comparing the surface [Cl^-] by microelectrodes to oocytes injected with known Cl^--dependent and -independent *slc4a*-derived transporters. The data pattern of the *SLC4A10*-injected oocytes was similar to the Cl^--independent transporters and different from known Cl^- extruders. Some of the inconsistencies may rely on differences between mammalian cells and *Xenopus* oocytes, temperature, and composition of solutions, the transfection/injection efficiency or molecular tagging of the transport proteins. Discrepancy in transport mode caused by the expression systems has previously been described for other members of the *slc4a* family, Nbce2 and Nbce1 (14–18). To circumvent these putative sources of error, we use stable transfection with incorporation of a single copy of untagged *slc4a10* into a predefined locus in a mammalian fibroblast cell line without native Na^+:HCO_3^- transport and performed all experiments at a temperature and in buffers that are appropriate for the mammalian protein.

In agreement with the studies by Wang *et al.* (2) and Giffard *et al.* (6), we find that *slc4a10*-induced transport is Cl^--dependent because as depletion of internal and external Cl^- completely inhibits pH_i recovery from acid values. We also find that acutely creating an outward chemical gradient for Cl^- enhances *slc4a10*-induced transport. This is indicative of Cl^- transport but does not rule out that the protein somehow senses a Cl^- gradient without transporting the ion. Finally, we found evidence for a Na^+-dependent, CO_2/HCO_3^--dependent, DIDS-sensitive Cl^- efflux in *slc4a10*-transfected cells in agreement with Wang *et al.* Importantly, this Cl^- efflux during pH_i recovery was not accompanied by detectable Cl^- influx. Analysis of the apparent Na^+:HCO_3^- stoichiometry was performed to support the functional coupling of Na^+:HCO_3^- to Cl^- efflux. The Na^+:HCO_3^- stoichiometry is supposed to be 1:2 or greater when *slc4a10* exchanges Cl^- for HCO_3^- to maintain the electroneutrality. It is noted that electroneutrality has been demonstrated by microelectrode recording of *SLC4A10*-injected *Xenopus* oocytes in just one study (7). We estimated a Na^+:HCO_3^- stoichiometry of 1:2 in *slc4a10*-transfected cells, whereas the apparent ratio in *slc4a7*-transfected cells was 1:1 (encoding the Cl^--independent electroneutral Na^+:HCO_3^- cotransporter Nbcn1).

There are more ways to explain the apparent transport of two HCO_3^-/Na^+ molecules: (i) two molecules of HCO_3^-, (ii) one molecule of CO_3^{2-}, or (iii) countertransport of H^+. The first two possibilities would require more than one positive amino acid in a given domain to attract and translocate the negative ion(s). Interestingly, the second large hinge-like loop between proposed TM11 and TM12 of *slc4a10* contained two such amino acids (His^{976} and His^{980}) and varies among *slc4a10*-derived proteins of varying transport mode. Mutations in each of these significantly reduced *slc4a10*-induced Na^+-dependent pH_i recovery, and double mutation of these amino acids hindered any transport. Mutations of the corresponding amino acid residues in Ae1 (Arg^{827} and Trp^{831}) led to identical degree of transport inhibition (8). Quadruple mutation of the specific charged amino acids in the hinge-like regions also completely prevented *slc4a10*-induced Na^+-dependent pH_i recovery. The reason for the observed decreases in *slc4a10* polypeptide function may be that the four charged amino acids are involved in the attraction or even the translocation of Na^+ and HCO_3^-. Certainly, the changes are not explained by variations in membrane abundance as judged from the surface biotinylation analysis. Major changes in protein folding are usually detected by the cellular quality control systems and are not likely to reach the plasma membrane. Nevertheless, smaller changes in tertiary structure may have been induced by these mutations. It is evident that many more residues of these polypeptides are involved in ion transport. As an example, Ser^{731} and His^{734} in the first hinge-like loop of Ae1 are conserved among more types of transporters. Single mutations of these residues deleted anion exchange but introduced cation leak (19). In this study, we focus on the amino acids that may underlie the variations in ionic requirement among the gene family members. The omission of charged amino acids, which are shared by the group of *slc4a* proteins known to transport more than one HCO_3^- molecule/Na^+, greatly affects transport by the *slc4a10*-derived protein. Thus, the mutational analysis would support that the *slc4a10* gene product belongs to this group of transporters.

In conclusion, we find that the *slc4a10* expression induces Na^+-dependent Cl^-/HCO_3^- exchange in a mammalian cell system with our experimental conditions, and we propose the protein name remains Ncbe. We speculate that the first hinge-like region is necessary for the Na^+ translocation process and the second for the HCO_3^- or CO_3^{2-} translocation process. Further structural analyses including crystallization of the transporter are necessary to determine fully the transport mode of Ncbe.

Acknowledgments—We thank Robert A. Fenton for guidance concerning transfection strategy and surface biotinylation and Christian Valdemar Westberg, Tina Drejer, and Helle Hoyer for expert technical assistance.

REFERENCES

1. Boron, W., and Boulpaep, E. L. (2009) *Medical Physiology*, 2nd Ed., pp. 667–671, W. B. Saunders Co., Philadelphia, PA
2. Wang, C. Z., Yano, H., Nagashima, K., and Seino, S. (2000) *J. Biol. Chem.* **275,** 35486–35490
3. Praetorius, J., Nejsum, L. N., and Nielsen, S. (2004) *Am. J. Physiol. Cell Physiol.* **286,** C601–C610
4. Jacobs, S., Ruusuvuori, E., Sipilä, S. T., Haapanen, A., Damkier, H. H., Kurth, I., Hentschke, M., Schweizer, M., Rudhard, Y., Laatikainen, L. M., Tyynelä, J., Praetorius, J., Voipio, J., and Hübner, C. A. (2008) *Proc. Natl. Acad. Sci. U.S.A.* **105,** 311–316
5. Gurnett, C. A., Veile, R., Zempel, J., Blackburn, L., Lovett, M., and Bowcock, A. (2008) *Arch. Neurol.* **65,** 550–553
6. Giffard, R. G., Lee, Y. S., Ouyang, Y. B., Murphy, S. L., and Monyer, H. (2003) *Eur. J. Neurosci.* **18,** 2935–2945
7. Parker, M. D., Musa-Aziz, R., Rojas, J. D., Choi, I., Daly, C. M., and Boron, W. F. (2008) *J. Biol. Chem.* **283,** 12777–12788
8. Zhu, Q., Lee, D. W., and Casey, J. R. (2003) *J. Biol. Chem.* **278,** 3112–3120
9. Praetorius, J., and Nielsen, S. (2006) *Am. J. Physiol. Cell Physiol.* **291,** C59–C67
10. Boyarsky, G., Ganz, M. B., Sterzel, R. B., and Boron, W. F. (1988) *Am. J. Physiol. Cell Physiol.* **255,** C844–C856
11. Damkier, H. H., Prasad, V., Hübner, C. A., and Praetorius, J. (2009) *Am. J. Physiol. Cell Physiol.* **296,** C1291–C1300
12. Damkier, H. H., Nielsen, S., and Praetorius, J. (2007) *Am. J. Physiol. Regul.*

Integr. Comp. Physiol. **293,** R2136–R2146
13. Moeller, H. B., Praetorius, J., Rützler, M. R., and Fenton, R. A. (2010) *Proc. Natl. Acad. Sci. U.S.A.* **107,** 424–429
14. Romero, M. F., Fong, P., Berger, U. V., Hediger, M. A., and Boron, W. F. (1998) *Am. J. Physiol. Renal Physiol.* **274,** F425–F432
15. Gross, E., Hawkins, K., Abuladze, N., Pushkin, A., Cotton, C. U., Hopfer, U., and Kurtz, I. (2001) *J. Physiol.* **531,** 597–603
16. Sassani, P., Pushkin, A., Gross, E., Gomer, A., Abuladze, N., Dukkipati, R., Carpenito, G., and Kurtz, I. (2002) *Am. J. Physiol. Cell Physiol.* **282,** C408–C416
17. Millar, I. D., and Brown, P. D. (2008) *Biochem. Biophys. Res. Commun.* **373,** 550–554
18. Virkki, L. V., Wilson, D. A., Vaughan-Jones, R. D., and Boron, W. F. (2002) *Am. J. Physiol. Cell Physiol.* **282,** C1278–C1289
19. Guizouarn, H., Martial, S., Gabillat, N., and Borgese, F. (2007) *Blood* **110,** 2158–2165